Honda Research Institute EU
Honda Research Institute Europe GmbH
https://www.honda-ri.de/

Risk-based Driver Assistance for Approaching Intersections of Limited Visibility

Florian Damerow, Tim Puphal, Julian Eggert

2017

Preprint:

This is an accepted article published in International Conference on Vehicular Electronics and Safety 2017. The final authenticated version is available online at: https://doi.org/10.1109/ICVES.2017.7991922

Risk-based Driver Assistance for Approaching Intersections of Limited Visibility

Florian Damerow[1], Tim Puphal[2], Yuda Li[1] and Julian Eggert[2]

***Abstract*— This work addresses the general problem of risk evaluation in traffic scenarios for the case of limited observability of the scene due to a restricted sensory coverage. Here we especially concentrate on intersection scenarios, which are visually difficult to access. To distinguish the area of sight, we employ publicly available digital map data which includes, besides the general road geometry, information about buildings potentially blocking the driver's visibility. Based on the estimated area of sight, we augment the sensory perceived environment with potentially present, but not perceivable, critical scene entities. For those potentially present scene entities, we predict a, for the ego driver, worst-case-like behavior and evaluate the upcoming collision risk. This risk model can then be employed to enrich the traffic scene analysis with potentially upcoming hazards, which result from a restricted sensory coverage. Furthermore, it can be utilized to evaluate the driver's current behavior in terms of risk, warn the driver in case its current behavior is considered as critical and give suggestions on how to act in a risk-aversive way. By applying the resulting intersection warning system to real world scenarios, we could validate our approach. The proposed system's behavior reveals to be highly similar to the general behavior of a correctly acting human driver.**

I. Introduction

In the past years many intelligent advanced driver assistance systems (ADAS) have been developed to detect upcoming obstacles and avoid collisions. Here, the forward area including dynamic road entities is generally captured by on-board sensors, such as radar or cameras. Based on the scene observation, upcoming hazards are determined to warn the driver or actively perform an evasive maneuver. As an example, adaptive cruise control (ACC) systems as in [1] detect leading vehicles, estimate upcoming collisions and adapt the ego driver's velocity to safely follow the leading vehicle.

Current intersection warning systems assess upcoming hazards purely based on the actual sensor input, but do not consider sensor limitations due to occlusion. For example [2] predicts the trajectories of all traffic participants on the intersection to determine their intersections and calculating the corresponding risk with time-to-collision (TTC).

To overcome narrow sensor ranges recent approaches, such as [3], rely on active systems integrated in the road infrastructure at intersections. Approaching vehicles, which are eventually undetectable by on-board sensors, are detected by the road infrastructure unit, e.g. by vehicle-to-infrastructure (V2I) communication, to then warn the individual drivers of upcoming collisions. However, such infrastructure units are often not present and most current traffic participants are not equipped with the necessary communication systems.

In this paper we propose a method to assess the risk with an ego vehicle's on-board sensor at intersections, where other approaching traffic entities are difficult to access. Therefore, we (1) estimate critical occluded areas, (2) model virtual vehicles with specific behaviors in those areas and (3) calculate their risk for the ego vehicle. The method is then applied to evaluate the driver's currently performed behavior when approaching an intersection of limited visibility to warn in case the behavior is considered as critical. Our intersection warning system considers sensor limitation and does not require additional hardware. In the next Section II, we introduce the functionality of our intersection warning system. In Section III, we validate the system with real world intersection scenarios and Section IV shows research areas for further improvement.

II. Collision Risk at Areas of Limited Visibility

A. Approach

Risks at intersections are generally caused by other traffic participants approaching the upcoming intersection. Depending on traffic rules the collision risk with each of the other involved entities has to be estimated by predicting their future behaviors. However, many areas around inner-city intersections are difficult to access by on-board sensors of the ego vehicle, as they are occluded e.g. by buildings. The collision risk with occluded traffic participants cannot be assessed directly. Consequently, the ego driver has to consider potentially present but sensorily not detectable entities and their assumed behaviors.

Taking this into consideration, a suitable ego vehicle's behavior would be slowing down when approaching an intersection of limited observability to be able to stop in case another non-detectable entity with right-of-way appears. Once the intersection can be accessed by the vehicle's sensors to an extent that a safe crossing can be ensured, the ego entity can keep on driving. Our approach mimics this concept and is shown with its individual steps in Fig. 1.

We first estimate the sensorily visible (non-occluded) area at an upcoming intersection, starting from the current position of the ego vehicle. Therefore, we use in a ray casting algorithm [4] the outline of buildings close to the intersection as occluding objects, which are gathered from

[1]Florian Damerow, Yuda Li are with the Control Methods and Robotics Lab, Technical University of Darmstadt, 64283 Darmstadt, Germany florian.damerow@continental-corporation.com

[2] Tim Puphal and Julian Eggert are with the Honda Research Institute (HRI) Europe, Carl-Legien-Str. 30, 63073 Offenbach, Germany tim.puphal@honda-ri.de, julian.eggert@honda-ri.de

©2017 IEEE. Personal use of this material is permitted.
Permission from IEEE must be obtained for all other uses, in any current or future media, including reprinting/republishing this material for advertising or promotional purposes, creating new collective works, for resale or redistribution to servers or lists, or reuse of any copyrighted component of this work in other works.
DOI: 10.1109/ICVES.2017.7991922

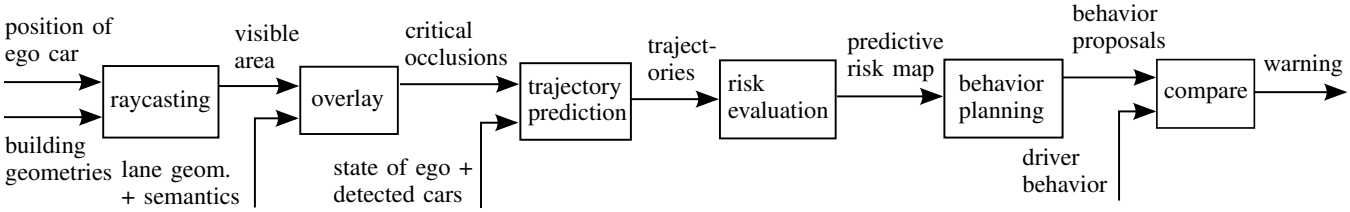

Fig. 1: Warning system for intersections of limited visibility by modeling virtual vehicles at occlusions.

OpenStreetMap data [5]. In the process, the sensor range is reduced by the building geometries.

Then, map data comprising lane-precise geometric and semantic information is used to extract those lanes, on which potentially critical entities might approach the intersection. The semantic information mainly defines how incoming lanes are connected to outgoing lanes. Potentially critical and thus relevant incoming lanes are e.g. lanes with right-of-way priority over the ego vehicles current lane. By overlaying map data, which contains the road topology of relevant incoming lanes, with the visible area, we can assess occluded lane segments with potential risk sources at the intersection. In those occluded areas we model virtual vehicles with specific behavioral assumptions. In this way, we can predict future spatio-temporal trajectories with employing constant velocity models [6]. This includes all virtual entities which are sensorily not detectable but potentially present as well as the ego entity. For all sensorily detected traffic participants, we use the so-called Foresighted Driver Model [7], which is interaction-aware and thus a more sophisticated prediction model.

A variation of possible ego behavior alternatives in combination with the predicted trajectories of all other involved entities (virtual and detected entities) are evaluated in terms of risk, to build so-called predictive risk maps [8].

A predictive risk map represents how risky a certain ego behavior alternative will be at a certain point in the future and can be used to plan risk-aversive future behaviors. Here, we calculate constant velocity, constant deceleration and constant acceleration trajectories through the risk map and propose those which represent risk-aversive behavior alternatives.

By comparing the driver's current behavior with the proposed behavior alternatives, we achieve an ADAS that is able to warn the driver in case the current behavior is not considered as safe due to critical occlusions. In addition, the most suitable risk-aversive behavior option can be communicated to the human driver. The individual steps are described more in detail in the following Sections II-B to II-F.

B. Estimation of Visible Area

The estimation of sensory observability, here especially the estimation of the visible area at intersections, is crucial for our approach to tackle the problem of the evaluation of risk caused by the lack of observability and thus caused by non-perceivable, but potentially present traffic scene entities.

There are multiple ways to estimate a driver's sensory observable area. E.g. in case of using a lidar sensor a three dimensional model for the environment [9] can be extracted, which again can be used to estimate the observable area. Furthermore with a stereo camera, object detection algorithms [10] can be utilized to detect other cars reducing the visible area.

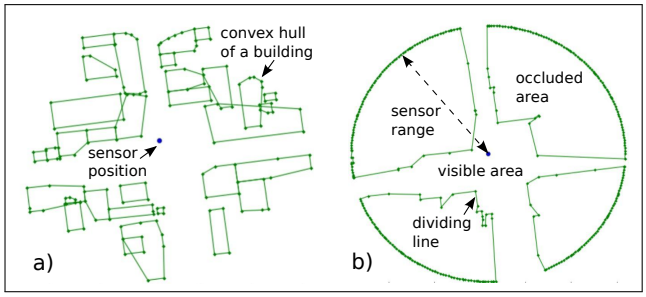

Fig. 2: Occlusion properties of buildings. a) Represented by its convex hull. b) After using the ray casting algorithm.

In this paper, we focus on static objects, such as buildings, as occluding objects. To some extent in accuracy, those objects can be extracted from publicly available map data, such as OpenStreetMap. In a preprocessing step we search for all buildings close to the upcoming intersection and afterwards represent each building by its ground plane's convex hull, as depicted for a toy example in Fig. 2 a). The convex hull is an efficient representation regarding the occultation properties of objects.

In order to find the region of visibility we start with the sensor's theoretical detection area. For simplicity we assume a circular detection area with a radius $r = 50\,\mathrm{m}$ around the current position of the sensor. In this area, we assume the sensor to provide reliable measurements for non-occluded areas. In a next step we use a ray casting algorithm, where we target only the corner points of the convex hull of each entity. As a result, we gain the multi-line that divides the visible area from the area occluded by each considered object. By geometrically subtracting the occluded areas of each object from the theoretically detectable area of the sensor we gather an estimate of the area that can be captured by the vehicle's sensor, as shown in Fig. 2 b).

C. Modeling of Virtual Cars

The goal of this system is to assess the upcoming risk to enable the evaluation of the current ego entity's behavior and allow the generation or planning of a risk-aversive future behavior. This implies the prediction of possible future scene evolutions including all captured traffic participants. Besides the sensorily captured entities, it is necessary to consider

©2017 IEEE. Personal use of this material is permitted.
Permission from IEEE must be obtained for all other uses, in any current or future media, including reprinting/republishing this material for advertising or promotional purposes, creating new collective works, for resale or redistribution to servers or lists, or reuse of any copyrighted component of this work in other works.
DOI: 10.1109/ICVES.2017.7991922

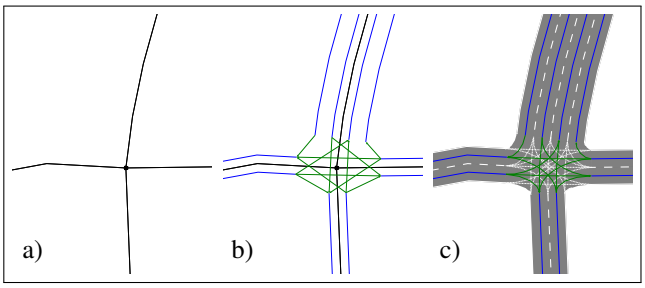

Fig. 3: Extension of OpenStreetMap data. a) Provided road geometries. b) Inferred lane semantics. c) Enrichment of detailed lane geometries.



Fig. 4: Example of a partially visible intersection. Left: Satellite view [11] and visibility area. Right: Positioning of a non-detectable but potentially critical virtual car.

entities, which cannot be detected by the vehicle's on-board sensors, but which potentially cause high risks for the ego vehicle, e.g. entities which approach the same intersection as the ego vehicle, but which are occluded by nearby buildings. Consequently, the system has to estimate possible positions, where such non-observable critical entities may be located and it also has to predict their future behavior.

OpenStreetMap provides only the center line of each road element and their intersection points. To estimate locations of potentially critical traffic entities we enhance OpenStreetMap data with semantic and geometric information on the lane level as shown in Fig. 3.

Subsequently, the lane semantics are used to determine all incoming lanes of the upcoming intersection. We select the relevant incoming lanes, which have right-of-way priority over the ego vehicle's current lane. By overlaying the visible area from Section II-B with the relevant lane geometries, we can achieve a geometric estimate of all those relevant lane segments which can not be captured by the vehicle's sensors.

Virtual traffic participants might be located anywhere in the occluded area of relevant lane segments with a highly uncertain behavior. Only a general human behavior when approaching an intersection considering the vehicle dynamics can be assumed. Instead of considering a virtual entity at every possible occluded position on all relevant lanes, we define for each relevant lane only one virtual entity located at the occluded position closest to the upcoming intersection.

Constant velocity models are used longitudinally along the considered lane's center line to predict a future scene evolution for the virtual entities (e.g. 40 km/h for inner-city intersections). Once the predicted position is located at the most critical position, right in the middle of the intersection, we assume a sudden stop in the trajectory prediction. This represents a worst-case-like behavior for the ego driver and enables a computationally inexpensive way to reproduce different positions and also, to some extend, velocity profiles of the virtual vehicles.

Fig. 4 illustrates the procedure of modeling critical virtual vehicles. It shows a green ego-car approaching an intersection. The visible area (orange) is limited due to occlusion caused by buildings (blue) and a virtual car (red) is located on the critical lane (light red) at the boundary of the visible area with a longitudinal velocity profile pointing to the intersection center.

D. Collision Risk Evaluation

Risk in general is the expectation value of the cost related to critical future events [**?**]. As a consequence, the evaluation of risk includes a prediction of events as well as an estimation of the damage in case a related critical event occurs.

In [12], a probabilistic model to assess a so-called event probability P_E, based on a survival analysis with the predicted spatio-temporal trajectories of all involved entities, is derived

$$P_E(s;t,\delta t) = S(s;t)\{\tau^{-1}(\text{states}(t+s))\delta t\}. \tag{1}$$

The survival function S thereby indicates the likelihood that an entity "survives" until a certain time $t+s$ in the future (current time t and future time $t+s$) and the total event rate τ^{-1} represents the likelihood for a critical event

$$S(s;t) = \exp\{-\int_0^s \tau^{-1}(\text{states}(t+s'))\,ds'\}, \tag{2}$$

$$\tau^{-1}(\text{states}(t+s')) = \sum_i \tau_i^{-1}(\text{states}_i(t+s)). \tag{3}$$

To cover different types of risk, the total event rate τ^{-1} can be composed of several types of single event rates τ_i^{-1}, such as car-to-car collision risk or the risk of skidding off the road in curves. Here, we consider only car-to-car collision risks represented by the single event rate τ_d^{-1} that is a function of the distance d of the ego car and the other considered traffic entity

$$\tau_d^{-1} = \tau_{d,0}^{-1}\exp\{-\beta_d(d-d_{min})\}. \tag{4}$$

Finally, by combining the probabilistic model with a deterministic damage model that uses the masses m and predicted velocities $\hat{v}$ of the two vehicles, we obtain a risk model which can be utilized to evaluate possible future evolutions of a currently sensed scene in a time-continuous way

$$\text{risk}(s) = P_E(s;0,\delta t)\,\text{damage}(\text{states}(s)), \tag{5}$$

$$\text{damage}(s) \sim \frac{1}{2}\frac{m_0 m_i}{m_0+m_i}[\hat{v}_0(s)-\hat{v}_i(s)]^2. \tag{6}$$

The risk model is used to build predictive risk maps, as shown in Fig. 5. In the process, we do not only calculate the risk along a defined path $\hat{l}^0$ for one predicted trajectory of the ego car $\hat{\mathbf{x}}^0$ with respect to the other car's predicted

©2017 IEEE. Personal use of this material is permitted.
Permission from IEEE must be obtained for all other uses, in any current or future media, including reprinting/republishing this material for advertising or promotional purposes, creating new collective works, for resale or redistribution to servers or lists, or reuse of any copyrighted component of this work in other works.
DOI: 10.1109/ICVES.2017.7991922

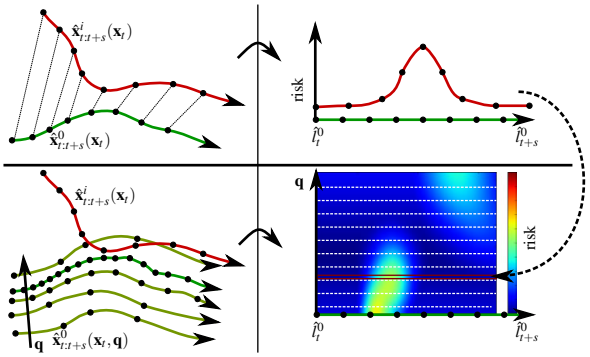

Fig. 5: Generation of a predictive risk map. Top: Use of risk model. Bottom: Variation of ego car's predicted velocities.

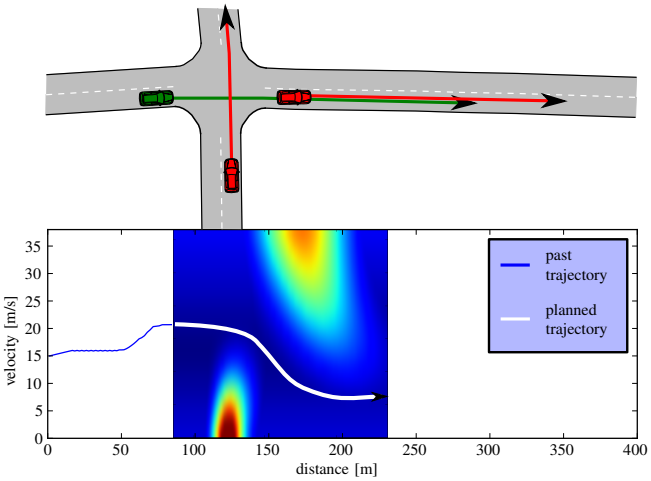

Fig. 6: Behavior planning using predictive risk maps. Top: Intersection scenario with two other cars. Bottom: Risk map with planned trajectory.

trajectory $\hat{\mathbf{x}}^i$. Instead, we create a set of ego car trajectories $\hat{\mathbf{x}}^0(\mathbf{q})$ defined by variation parameters $\mathbf{q}$ and evaluate the risk for each trajectory. When we use the predicted ego car velocity $\hat{v}_0$ as $\mathbf{q}$, a predictive risk map can be composed, which indicates how risky a chosen ego velocity will be for the predicted time $t+s$.

E. Planning of Risk-aversive Behaviors

With predictive risk maps the evaluation of future behavior alternatives for the ego vehicle in terms of collision risk is possible. A modified, globally optimizing version of the rapidly-exploring random tree search algorithm (RRT*) has been used in [13] to plan the best possible velocity profile as a "path" through predictive risk maps, minimizing risk and maximizing utility considerations. Fig. 6 displays the outcome of the algorithm for an intersection scenario with two other traffic entities. The future cost-optimized trajectory swerves around the two corresponding collision risk points in the risk map.

To fulfill computation time constraints we use a planning algorithm of reduced complexity to generate behavior proposals by only considering the three behavior alternatives: 1) keep on driving with constant velocity, 2) brake with constant deceleration to be able to stop at the stop line of the intersection and 3) accelerate with constant acceleration to safely pass in front of the non-detectable approaching vehicle.

In a first step, the three behavior alternatives have to be calculated. Each is represented by a deceleration/acceleration value. For driving with constant velocity, we can set

$$a_{\text{const}} = 0\,\text{m/s}^2. \tag{7}$$

The deceleration that is needed to stop at the stop line is calculated according to

$$a_{\text{stop}} = -\frac{v_0^2}{2\ d_{\text{sl}}}, \tag{8}$$

where v_0 is the current ego car velocity and d_{sl} the distance to the intersection entry point or stop line. The distance d_{sl} is derived from our map data introduced in II-C.

For passing in front of potentially approaching vehicles, we use the risk map to estimate the target velocity v_{trg} that has to be reached at the intersection to pass with a certain low risk value. The required acceleration is then

$$a_{\text{acc}} = \frac{v_{\text{trg}}^2 - v_0^2}{2\ d_{\text{cp}}}, \tag{9}$$

with d_{cp} as the distance to the expected crossing point on the intersection between the expected ego- and the other vehicle's path.

In a second step, we evaluate the three behavior alternatives a_{const}, a_{stop} and a_{acc} in the risk map. Hereby, not only the collision risk from virtual vehicles, but also from detected vehicles by the vehicle's sensors are depicted in the risk map and have priority over occlusion risks. In case the resulting risk value is above some threshold, the behavior alternative is neglected and not considered as a suitable action. In this way, the remaining behavior alternatives are generally of low risk and can be called risk-aversive behaviors.

In [14] a situation classification is placed in front of the behavior planning to consider different possible interactions of the traffic participants. The proposed approach for occlusion risk can seamlessly be incorporated into this full behavior planning framework.

F. Driver Warning and Behavior Suggestion

The ADAS functionality should only step in, when the currently performed behavior of the human driver is critical. For that purpose, we categorize the planned risk-aversive behaviors a_{const}, a_{stop} and a_{acc} in four levels of intervention according to Fig. 7: comfortable (green), heavy (yellow), emergency (red) and non-reachable (gray) [15].

It can be seen that a_{const} always lies in the comfortable area. However, the values of a_{stop} and a_{acc} can vary depending on the current appearance of the risk map and thus reach different levels of intervention. We define that if both a_{stop} and a_{acc} have left the comfortable region, the driver behavior is seen as critical. When using them, the car would come near its physical limits. If a_{stop} or a_{acc} are even in the non-reachable area, they have to be disregarded because it is not possible to execute them.

©2017 IEEE. Personal use of this material is permitted.
Permission from IEEE must be obtained for all other uses, in any current or future media, including reprinting/republishing this material for advertising or promotional purposes, creating new collective works, for resale or redistribution to servers or lists, or reuse of any copyrighted component of this work in other works.
DOI: 10.1109/ICVES.2017.7991922

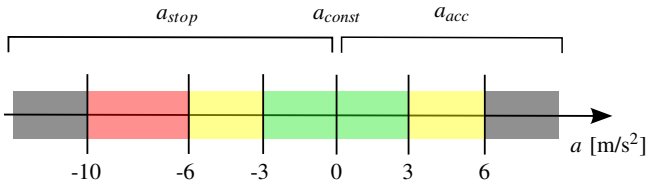

Fig. 7: Levels of necessary braking or accelerating [15]

In compliance with the definition of driver criticality, we display a warning if a_{const} is not safe (not among the proposed actions) and

$$a_{stop} \leq -3\,\text{m/s}^2 \quad \wedge \quad a_{acc} \geq 3\,\text{m/s}^2. \tag{10}$$

Additionally, at this point the behavior option with the lowest level of intervention can be provided to the driver.

Is the driver not appropriately responding to the warning, it is possible that a control mode gets activated. As shown in Fig. 7, we do not consider a_{acc} as an appropriate emergency action. But if the best possible action (lowest level of intervention) is a_{stop} in the emergency area

$$-10\,\text{m/s}^2 \leq a_{stop} \leq -6\,\text{m/s}^2, \tag{11}$$

the system could intensify the warning at first and then after waiting a certain time period initiate an emergency brake.

III. Results on Real World Scenarios

We applied the presented ADAS for approaching intersections which are hard to access by the vehicle's on-board sensors to real world scenarios taken from the KITTI dataset [16]. The behavior of the human driver can usually be considered as safe in this dataset. To evaluate driver behavior which can be considered as critical, we chose scenarios where the ego vehicle is actually on a priority road. However, we neglect the priority information. This results in a behavior, where the driver crosses intersections of limited visibility while neglecting potentially approaching but not detectable vehicles.

A. Scenario with Safe Human Behavior

Fig. 8 outlines at the top a satellite view of the ego vehicle approaching a partially visible intersection due to buildings to the right. Below, the modeling of the virtual car and the corresponding risk maps are shown for three consecutive time steps represented with the traveled distance $d = [84, 118, 126]$m. Besides depicting the risks from the modeled virtual cars at occlusions, the plot also indicates the actually driven velocity profile of the human driver (purple line), the velocity profiles of the proposed behaviors a_{const}, a_{stop} and a_{acc} (yellow lines), the position of the stop line at the intersection d_{sl} (white vertical line) and the velocity that is necessary at the collision point to pass in front of any potentially non-detectable vehicle v_{trg} (black horizontal line).

Out of the concatenation of a_{const}, a_{stop} and a_{acc} two risk-minimizing/safe trajectories can be derived, which are plotted with the intervention levels in Fig. 9. The three time steps

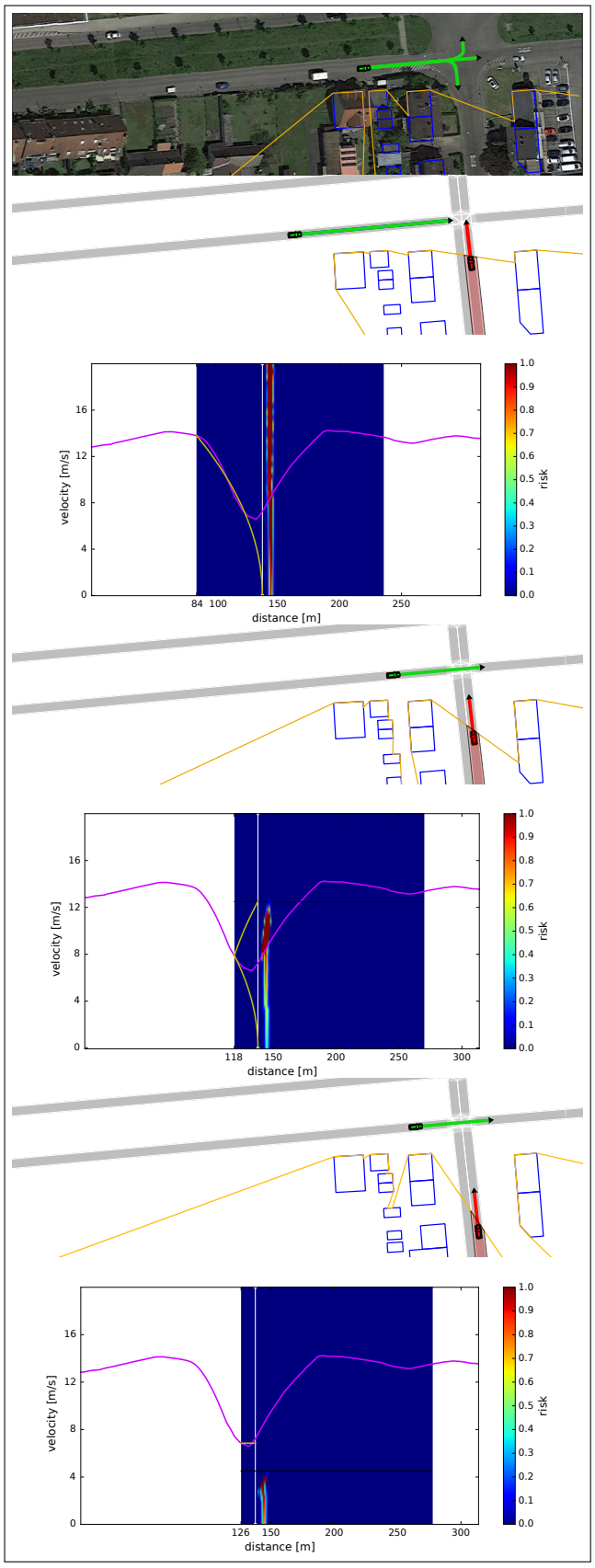

Fig. 8: Evaluation of intersection assistance for limited visibility using a scenario with correct human behavior. Top: Satellite view and visibility area. Bottom: Simulation view and risk maps.

©2017 IEEE. Personal use of this material is permitted.
Permission from IEEE must be obtained for all other uses, in any current or future media, including reprinting/republishing this material for advertising or promotional purposes, creating new collective works, for resale or redistribution to servers or lists, or reuse of any copyrighted component of this work in other works.
DOI: 10.1109/ICVES.2017.7991922

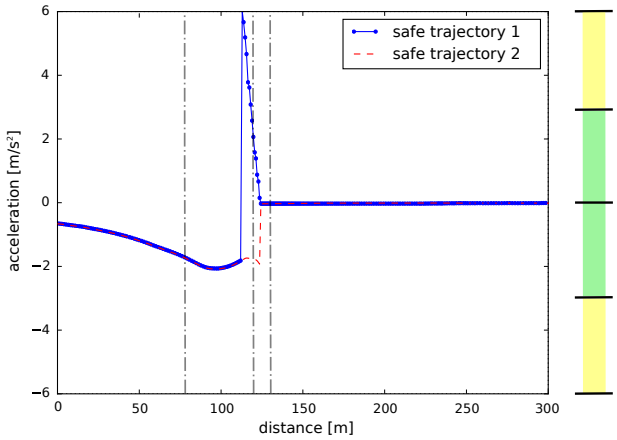

Fig. 9: Possible safe trajectories ranked by intervention level for a scenario with correct human behavior.

are marked in the plot with three dashed vertical gray lines.

In this case the human behavior can be considered as safe. The driver slows down until the intersection is mostly visible and accelerates back to the desired cruising velocity. Consequently, he/she is always able to safely stop at the stop line in case a car occurs from the occluded area.

At $d = 84\,\mathrm{m}$ the intersection is largely occluded, but the stop line is still $d_{\mathrm{sl}} = 50\,\mathrm{m}$ away. A deceleration of $a_{\mathrm{stop}} = -1\,\mathrm{m/s^2}$ is proposed so that the velocity profile in the risk map avoids the risk spot.

When the ego vehicle is closer to the intersection with $d_{\mathrm{sl}} = 15\,\mathrm{m}$ at $d = 118\,\mathrm{m}$, the required deceleration increases to $a_{stop} = -2\,\mathrm{m/s^2}$. At the same time, the intersection is visible to such an extent that an acceleration of $a_{\mathrm{acc}} = 6\,\mathrm{m/s^2}$ would allow to pass the intersection in front of the virtual car by reaching $v_{\mathrm{trg}} = 12\,\mathrm{m/s}$. Since $a_{\mathrm{acc}} = 6\,\mathrm{m/s^2}$ is in the heavy intervention level, $a_{\mathrm{stop}} = -2\,\mathrm{m/s^2}$ is the recommended behavior. If a real vehicle appears from the non-visible area, by executing $a_{\mathrm{stop}} = -2\,\mathrm{m/s^2}$ the ego vehicle would be able to safely stop at the stop line without a collision.

Finally at $d = 126\,\mathrm{m}$, the intersection is nearly completely visible. Keeping the velocity constant with $a_{\mathrm{const}} = 0\,\mathrm{m/s^2}$ would not result in any potential collision anymore.

In all time steps the proposed behavior resembles the actual safe human behavior. The slope of one of the yellow and of the purple curve always have approximately the same value. Hence, the needed deceleration a_{stop} stays small and at no time a warning is triggered.

B. Scenario with Critical Human Behavior

Fig. 10 and 11 depict the simulation results of the ego vehicle approaching an intersection with an occluded incoming lane with priority over the ego vehicle's lane for three time frames $d = [58, 72, 86]\mathrm{m}$. The driver does not reduce the speed while coming closer to the intersection, effectively not considering potential related hazards. The driver behavior is seen as critical.

At $d = 58\mathrm{m}$ the ego velocity has a high value of $v_0 = 14\,\mathrm{m/s}$ so that a braking maneuver with $a_{\mathrm{stop}} = -3\,\mathrm{m/s^2}$ is

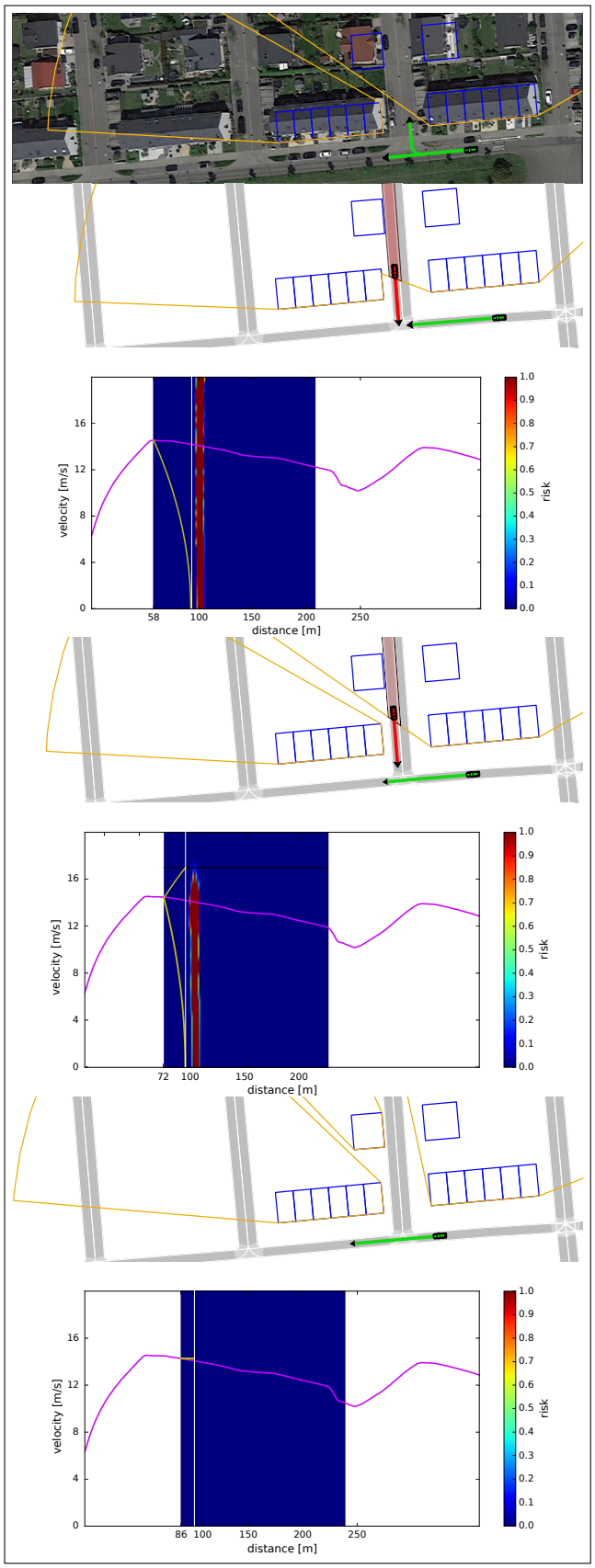

Fig. 10: Evaluation of intersection assistance for limited visibility using a scenario with incorrect human behavior. Top: Satellite view and visibility area. Bottom: Simulation view and risk maps.

©2017 IEEE. Personal use of this material is permitted.
Permission from IEEE must be obtained for all other uses, in any current or future media, including reprinting/republishing this material for advertising or promotional purposes, creating new collective works, for resale or redistribution to servers or lists, or reuse of any copyrighted component of this work in other works.
DOI: 10.1109/ICVES.2017.7991922

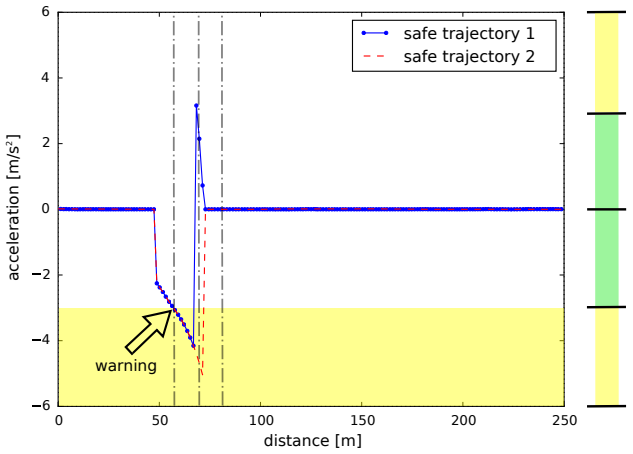

Fig. 11: Possible safe trajectories ranked by intervention level for a scenario with incorrect human behavior.

necessary to come to a safe halt in $d_{\text{sl}} = 30\,\text{m}$. Because $a_{\text{stop}} = -3\,\text{m/s}^2$ is the only behavior alternative and lies in the heavy intervention level, a warning is indicated to the driver.

Shortly after at $d = 72\text{m}$, the braking distance decreases to $d_{\text{sl}} = 16\,\text{m}$ whereas the velocity stays the same with $v_0 = 14\,\text{m/s}$, leading even to $a_{\text{stop}} = -5\,\text{m/s}^2$. At this point, it would be easier to avoid the risk spot by accelerating to $v_{\text{trg}} = 17\,\text{m/s}$ with $a_{\text{acc}} = 3\,\text{m/s}^2$. But since $v_{\text{trg}} = 17\,\text{m/s} > 50\,\text{km/h}$ which is the maximum allowed speed in inner-cities, $a_{\text{acc}} = 3\,\text{m/s}^2$ is neglected and a warning is still displayed.

In this example, there is no real car on the right lane. The intersection becomes entirely visible at $d = 86\text{m}$ and thus the risk map does not show a risk spot anymore. Driving with constant velocity $a_{\text{const}} = 0\,\text{m/s}^2$ is proposed to the driver without a warning.

In the first two time steps the behavior suggestion deviates from the actual human behavior. The slope of the yellow and purple curves have different values. When a_{stop} reaches the heavy intervention level, the system determines a critical driver behavior and gives a warning about 3s before a possible crash.

IV. Discussion and Outlook

In this work, we introduced a novel intersection warning system that not only allows the evaluation of collision risks from vehicles detected by the on-board sensor, but also risks originating from hypothetical cars appearing at occlusions, to plan risk-aversive behaviors. The sensor's visibility area to look into the upcoming intersection for dynamic road entities is thus virtually enhanced. Apart from map data to calculate the visible area, no information from additional sensors is needed.

Simulations showed that the proposed system's behavior is matching the general behavior of a correctly acting human driver. In scenarios where the actual human behavior is differing to the proposed behaviors of the system, a warning can be released to successfully avoid potential hazards lying at areas which cannot be accessed by the on-board sensor. Optionally, it is possible to display the safe trajectory with the lowest intervention level.

Currently, occlusions only result from buildings around the intersection. The sensor range can additionally be reduced by other static objects, such as parked cars and trees on the side, or by driving cars nearby. Also, the assumed behavior of the virtual entity just matches cars, but not pedestrians or bicyclists. It remains to be evaluated whether improvements in the fidelity of the occlusion risk calculation can be made.

In the planning of necessary braking and accelerating maneuvers, human factors, e.g. driving experience, have not been integrated yet. At the same time, it may be that one or more proposed behavior alternatives are not executable because they would violate traffic rules. Future research will concentrate on incorporating realistic driver types, so that a personalization of warning can be achieved.

Acknowledgments

This work has been supported by the European Unions Horizon 2020 project VI-DAS, under the grant agreement number 690772.

References

[1] H. Winner and M. Schopper, in *Handbuch Fahrerassistenzsysteme - Grundlagen, Komponenten und Systeme für aktive Sicherheit und Komfort*, 2015, pp. 478–521.

[2] O. Aycard, Q. Baig, S. Bota, F. Nashashibi, S. Nedevschi, C. Pantilie, M. Parent, P. Resende, and T.-D. Vu, "Intersection Safety using Lidar and Stereo Vision sensors," in *Intelligent Vehicles Symposium*, 2011, pp. 863–869.

[3] S. Andrews, "Intersection warning system," Patent, 1999, US Patent 5926114.

[4] L. Barba, M. Korman, S. Langerman, and R. I. Silveira, "Computing a visibility polygon using few variables," in *Journal of Computational Geometry*, 2011.

[5] OpenStreetMap Contributors, accessed: 2016-01-10. [Online]. Available: www.openstreetmap.org

[6] S. Lefevre, D. Vasquez, and C. Laugier, "A survey on motion prediction and risk assessment for intelligent vehicles," in *ROBOMECH Journal*, 2014.

[7] J. Eggert, F. Damerow, and S. Klingelschmitt, "The Foresighted Driver Model," in *Intelligent Vehicles Symposium*, 2015.

[8] F. Damerow and J. Eggert, "Predictive Risk Maps," in *Intelligent Transportation Systems Conference*, 2014, pp. 703–710.

[9] S. Thrun, M. Montemerlo, S. Strohband, C. Dupont, G. Bradski, and P. Mahoney et al., "Stanley: The Robot that Won the DARPA Grand Challenge," in *Journal of Field Robotics*, 2006, pp. 661–692.

[10] P. Sermanet, D. Eigen, X. Zhang, M. Mathieu, R. Fergus, and Y. LeCun, "OverFeat: Integrated Recognition, Localization and Detection using Convolutional Networks," in *International Conference on Learning Representations*, 2014.

[11] Google Maps Contributors, accessed: 2016-01-10. [Online]. Available: www.google.de/maps

[12] J. Eggert, "Predictive Risk Estimation for Intelligent ADAS Functions," in *Intelligent Transportation Systems Conference*, 2014, pp. 711–718.

[13] F. Damerow and J. Eggert, "Balancing Risk against Utility: Behavior Planning using Predictive Risk Maps," in *Intelligent Vehicles Symposium*, 2015.

[14] F. Damerow and J. Eggert, "Risk-Aversive Behavior Planning under Multiple Situations with Uncertainty," in *Intelligent Transportation Systems Conference*, 2015.

[15] H. Burg and A. Moser, in *Handbuch Verkehrsunfallrekonstruktion*, 2009, pp. 421–433.

[16] A. Geiger, P. Lenz, C. Stiller, and R. Urtasun, "Vision meets Robotics: The KITTI Dataset," in *International Journal of Robotics Research*, 2013.

©2017 IEEE. Personal use of this material is permitted.
Permission from IEEE must be obtained for all other uses, in any current or future media, including reprinting/republishing this material for advertising or promotional purposes, creating new collective works, for resale or redistribution to servers or lists, or reuse of any copyrighted component of this work in other works.
DOI: 10.1109/ICVES.2017.7991922